Thermoreflectance spectra of rf-sputtered epitaxial single-crystal films of $Pb_xSn_{1-x}Te$

Giorgio Cappuccio and Carlo Corsi
*Laboratorio di Elettronica dello Stato Solido del Consiglio Nazionale delle Ricerche, Gruppo Nazionale di Struttura della Materia, Roma, Italy**

Anita Giansantelli, Martino Grandolfo, and Claudio Ranghiasci
Physics Laboratory, Istituto Superiore di Sanità, Roma, Italy†
(Received 10 June 1976)

Thermoreflectance spectra of radio-frequency sputtered epitaxial single-crystal films of $Pb_{0.83}Sn_{0.17}Te$ from 1.5 to 6.0 eV, at room temperature and 100 K, have been measured and studied. $\Delta\epsilon_1$ and $\Delta\epsilon_2$ have been obtained through a Kramers-Kronig analysis of the experimental room-temperature $\Delta R/R$ spectra. A line-shape analysis of the E_2 structure has been performed in conjunction with an exact derivative procedure of the interband dielectric function at Van Hove singularities. Temperature coefficients have been measured and reported.

I. INTRODUCTION

For more than twenty years the lead-sulfide group has been the subject of considerable research effort, due both to the technological importance of these materials as detectors of infrared radiation, and to the interest in the basic physics of these narrow-gap semiconductors.[1]

Lead salts are extremely interesting semiconductors, exhibiting properties which are unusual, and probably unique, relative to other semiconductors, as reported by various review articles and papers.

Much information about the band properties of lead chalcogenides has been obtained by means of electrical,[2,3] optical[4,5] magneto-optical,[6] cyclotron-resonance,[7] recombination radiation,[8] pressure measurements,[9] and photoemission studies.[10] Energy-band parameters near the fundamental absorption edges based on the above measurements and reflectivity measurements for higher-lying transitions, permitted band-structure calculations which have given a fairly extensive picture of the energy-band structure of these materials.[4,11-17]

Modulation techniques have been employed in recent years in studying the band structure of semiconductors, yielding much greater sensitivity and resolution than that obtainable in direct measurements of the reflectance.[18] Because of their high dielectric constants and high carrier concentration, in the IV-VI compounds the inherent difficulties of extracting meaningful line shapes from electroreflectance derivative techniques are very much enhanced, and owing to the simplicity of analyzing experimental results, scalar first derivative techniques such as wavelength-modulated reflectance and thermoreflectance are especially appealing for studying critical points in the energy-band structure of these materials.[18,19] Epitaxial IV-VI films are moreover especially suited for thermoreflectance measurements since temperature modulation is achieved simply by varying the current through the samples.

Previous modulation optical studies of interband transitions of the $Pb_xSn_{1-x}Te$ alloy system are sparse. Electroreflection measurements were performed on the $Pb_xSn_{1-x}Te$ ternary compounds by Seraphin,[20] who found however electroreflectance spectra of $Pb_xSn_{1-x}Te$ to be extremely sensitive to dc bias, modulation depth, and modulation frequency. These difficulties have been circumvented using a wavelength-modulation-derivative-reflectivity technique, as recently shown by Korn and Braunstein.[21]

In this work we have measured, for the first time, the thermoreflectance spectra of $Pb_xSn_{1-x}Te$ alloy films grown epitaxially by radio-frequency sputtering technique, from 1.5 to 6 eV at room and liquid-nitrogen temperatures. The resulting $\Delta R/R$ was used to obtain $\Delta\epsilon_1$ and $\Delta\epsilon_2$ through Kramers-Kronig analysis. We focused our attention on the prominent E_2 structure present in reflectivity spectra, identified with the critical points in the energy-band structure of these compounds on the basis of the exact derivative treatment of the interband dielectric function at Van Hove singularities reported by Rabii and Fischer,[22] and more recently by Mondio, Saitta, and Vermiglio.[23]

II. THEORY

In order to investigate the modulated-reflectance line shapes associated with different critical points in scalar first-derivative spectra, Batz[19] considered only that part of the dielectric function $\epsilon(\omega)$ that most strongly contributes to the derivative spectrum, namely,

$$\epsilon(\omega) \sim i^{l+1}(\omega - \omega_g)^{1/2}, \quad (1)$$

where l is the order of the critical point and ω_g the corresponding energy-gap value. The real and imaginary parts of the derivative of Eq. (1) were expressed as a function of the dimensionless variable $x=(\omega-\omega_g)/\Gamma$ after introducing a phenomenological broadening parameter Γ. To explain the line shapes obtained in wavelength and thermal modulation experiments, the resulting "universal functions" were then used.[19] The hyperbolic exciton theory of Toyozawa *et al.*[28] was invoked to explain the mixing of different critical-point line shapes, when the experimental ones did not fit the universal functions.

Recently Rabii and Fischer[22] examined the effect of neglecting the nonresonant terms present in the dielectric function, finding many significative differences between the approximate universal line-shape functions and those obtained by exact derivative calculations. One of the major conclusion is that wavelength and temperature modulation no longer have identical line shapes. In their paper, Rabii and Fisher examined the effect of neglected terms on the derivatives of the complex dielectric function with respect to wavelength, $d\epsilon/d\omega$, obtaining results directly applicable to wavelength modulation and to the modulation of the broadening energy Γ, $d\epsilon/d\Gamma$, but not to energy gap modulation, $d\epsilon/d\omega_g$, which is the most important mechanism in giving rise to temperature-modulated optical spectra.

In order to interpret our derivative spectra obtained by thermal modulation we performed the first derivative of the exact interband complex dielectric function with respect to ω_g. As a result of this calculation we obtained the exact line shapes of the quantities $d\epsilon_1/d\omega_g$ and $d\epsilon_2/d\omega_g$ for the four different types of critical points.

The complex dielectric function near a three-dimensional M_l Van Hove singularity,[27] in the random-phase approximation, is

$$\epsilon(\omega)-1\simeq[-i^{l+1}/(\omega+i\Gamma)^2][2i(\omega_g)^{1/2}-(-\omega_g+\omega+i\Gamma)^{1/2}-i(\omega_g+\omega+i\Gamma)^{1/2}]. \tag{2}$$

To obtain the first derivative of the real and imaginary parts of Eq. (2) with respect to ω_g it is useful to rearrange the previous equation in the form

$$\begin{aligned}\epsilon(\omega)-1&=-i^{l+1}\{[\gamma_1(\omega)F_r(\omega)+\gamma_2(\omega)F_i(\omega)]\\&\quad+i[\gamma_1(\omega)F_i(\omega)-\gamma_2(\omega)F_r(\omega)]\}\\&=-i^{l+1}[B(\omega)+iA(\omega)],\end{aligned} \tag{3}$$

where

$$\gamma_1(\omega)=(\omega^2-\Gamma^2)/(\omega^2+\Gamma^2)^2;$$

$$\gamma_2(\omega)=2\omega\Gamma/(\omega^2+\Gamma^2)^2;$$

$$F_r(\omega)=-\left(\tfrac{1}{2}\{(\omega-\omega_g)+[(\omega-\omega_g)^2+\Gamma^2]^{1/2}\}\right)^{1/2}+\left(-\tfrac{1}{2}\{(\omega+\omega_g)+[(\omega+\omega_g)^2+\Gamma^2]^{1/2}\}\right)^{1/2};$$

$$F_i(\omega)=2\sqrt{\omega_g}-\left(-\tfrac{1}{2}\{(\omega-\omega_g)+[(\omega-\omega_g)^2+\Gamma^2]^{1/2}\}\right)^{1/2}-\left(\tfrac{1}{2}\{(\omega+\omega_g)+[(\omega+\omega_g)^2+\Gamma^2]^{1/2}\}\right)^{1/2};$$

and the prefactor $-i^{l+1}$ assumes the values $-i$, 1, i, -1, for the four kinds of critical points, M_0 to M_3, respectively. The functional dependences of quantities $F_r(\omega)$, $F_i(\omega)$, $A(\omega)$, and $B(\omega)$ versus the dimensionless variable $\hbar(\omega-\omega_g)/\Gamma$ are shown in Fig. 1, for the particular case $\omega_g=1.0$ eV, $\Gamma=0.01$ eV.

In order to evaluate the first derivative of Eq. (3) we recall that

$$\begin{aligned}\frac{\partial A(\omega)}{\partial\omega_g}&=\gamma_1(\omega)\frac{\partial F_i(\omega)}{\partial\omega_g}-\gamma_2(\omega)\frac{\partial F_r(\omega)}{\partial\omega_g},\\\frac{\partial B(\omega)}{\partial\omega_g}&=\gamma_1(\omega)\frac{\partial F_r(\omega)}{\partial\omega_g}+\gamma_2(\omega)\frac{\partial F_i(\omega)}{\partial\omega_g},\end{aligned} \tag{4}$$

where a straightforward calculation permits one to obtain the results:

$$\begin{aligned}\frac{\partial F_r(\omega)}{\partial\omega_g}&=\frac{1}{2}\left[\left(\frac{(\omega-\omega_g)+[(\omega-\omega_g)^2+\Gamma^2]^{1/2}}{2}\right)^{1/2}\frac{1}{[(\omega-\omega_g)^2+\Gamma^2]^{1/2}}\right.\\&\quad\left.-\left(\frac{-(\omega+\omega_g)+[(\omega+\omega_g)^2+\Gamma^2]^{1/2}}{2}\right)^{1/2}\frac{1}{[(\omega+\omega_g)^2+\Gamma^2]^{1/2}}\right],\\\frac{\partial F_i(\omega)}{\partial\omega_g}&=\frac{1}{\sqrt{\omega_g}}-\frac{1}{2}\left[\left(\frac{-(\omega-\omega_g)+[(\omega-\omega_g)^2+\Gamma^2]^{1/2}}{2}\right)^{1/2}\frac{1}{[(\omega-\omega_g)^2+\Gamma^2]^{1/2}}\right.\\&\quad\left.+\left(\frac{(\omega+\omega_g)+[(\omega+\omega_g)^2+\Gamma^2]^{1/2}}{2}\right)^{1/2}\frac{1}{[(\omega+\omega_g)^2+\Gamma^2]^{1/2}}\right].\end{aligned} \tag{5}$$

In Fig. 2 the exact derivatives $d\epsilon_1/d\omega_g$ and $d\epsilon_2/d\omega_g$ obtained for the four critical points by taking into account the results of Eqs. (4) and (5) are shown, for the above-mentioned particular case $\omega_g=1.0$ eV and $\Gamma=0.01$ eV.

III. EXPERIMENTAL

The experimental arrangement which has been used is the standard one in the technique of temperature-modulated solid-state spectroscopy.[19,24]

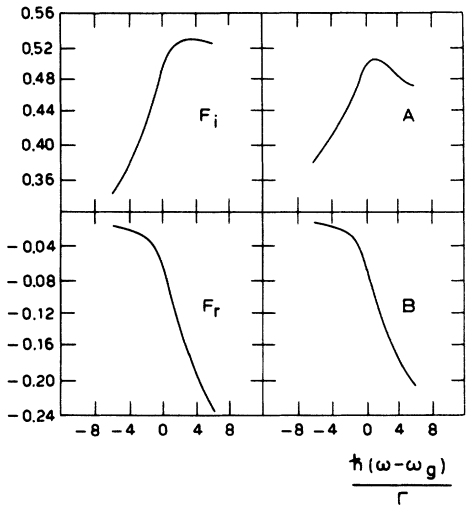

FIG. 1. Spectral dependence of functions $F_r(\omega)$, $F_i(\omega)$, $A(\omega)$, and $B(\omega)$ versus the dimensionless variable $\hbar(\omega-\omega_g)/\Gamma$. Curves are computed for $\omega_g = 1.0$ eV and $\Gamma = 0.01$ eV.

Light from a xenon lamp was focused on the entrance slit of a double-grating monochromator. The monochromatic light was focused on the sample, reflected at an angle of about 8°, and refocused on a photomultiplier. The dc portion of the output current from the photomultiplier, proportional to the reflectance of the sample R, was kept constant throughout the experiment. The ac component, proportional to the reflectance change ΔR induced by the periodic temperature modulation, was detected by a lock-in amplifier, whose reference signal was supplied by the same wave generator that determines the modulation frequency (7.7 Hz) and supplies power to heat the sample.

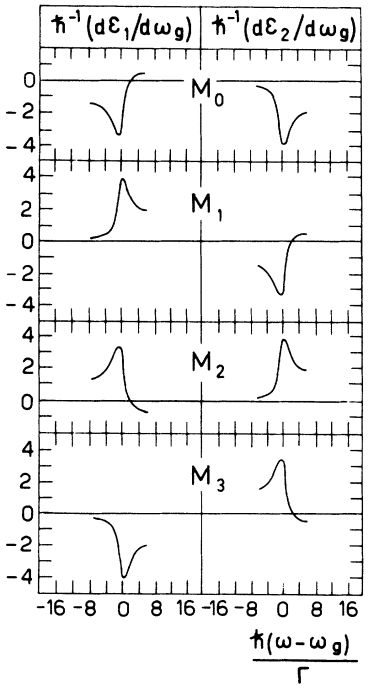

FIG. 2. Exact line shapes for the four types of three-dimensional Van Hove singularities. Curves are computed for $\omega_g = 1.0$ eV and $\Gamma = 0.01$ eV.

A multicathode rf-sputtering system, capable of simultaneous or sequential sputtering from three different targets, was used to deposit $Pb_xSn_{1-x}Te$ layers.[25,26] This system allowed us to deposit high-crystalline-quality films on large substrate areas. The nucleation and growth of the $Pb_xSn_{1-x}Te$ films took place via the mechanism of heteroepitaxial growth. Evidence for epitaxial growth has been obtained by Laue diffractometry, electron diffraction, and Debye-Scherrer methods. Thermoreflectance spectra were obtained on epitaxial films of composition $Pb_{0.83}Sn_{0.17}Te$ obtained on (111) BaF_2 substrates held at a temperature of 340 °C. These films presented an n-type conductivity, with carrier concentration of 1.5×10^{17} cm^{-3} and carrier mobility of 1.3×10^4 cm^2/V sec. Ohmic contacts have been obtained by evaporating gold electrodes on the substrates before the deposition of $Pb_xSn_{1-x}Te$ films. For the temperature modulation an indirect heating system was then employed by passing square-wave current pulses through these electrodes. The BaF_2 substrate acted as a heat sink when mounted on the copper cold finger of a metal cryostat fitted with quartz windows. The dc temperature of the samples was measured by a thermocouple attached to their surfaces, away from the incoming light beam; a value of about 100 K was measured. The amplitude of the temperature modulation ΔT, although not accurately measured in our experiment, did not exceed 3 K.

IV. EXPERIMENTAL RESULTS AND DISCUSSION

The thermoreflectance spectra $\Delta R/R$ for the $Pb_{0.83}Sn_{0.17}Te$ sample studied are shown in Fig. 3. For comparison, the absolute reflectivity spectrum of $Pb_{0.83}Sn_{0.17}Te$ is shown as measured by Korn and Braunstein[21] at room temperature and in the same spectral region; four peaks are labeled $E_1 - E_3$ according to convention of Ref. 4. Except the E_1 structure, which is beyond the energy range of our experimental apparatus, all other peaks are strictly correlated to structures present in our $\Delta R/R$ results. In Fig. 3 it is possible to observe the characteristic pattern in which reflectivity responds to the temperature changes.

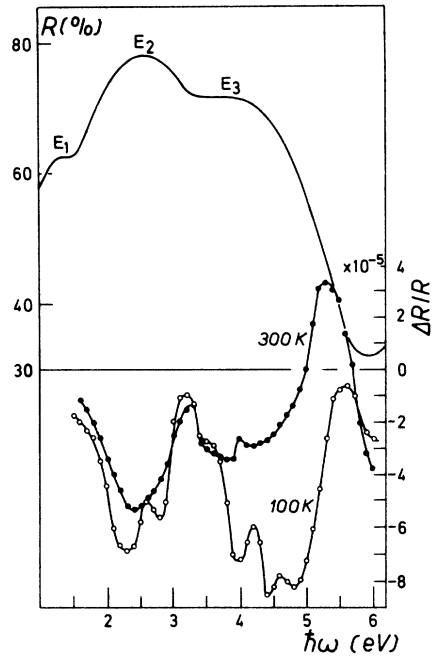

FIG. 3. Room-temperature absolute reflectivity spectrum (Ref. 21), and thermoreflectance spectra $\Delta R/R$ of rf-sputtered epitaxial single-crystal films of $Pb_{0.83}Sn_{0.17}Te$.

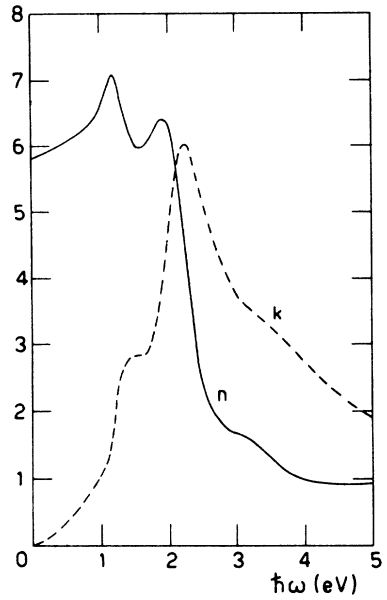

FIG. 4. Spectral dependence of the optical constants n and k for $Pb_{0.83}Sn_{0.17}Te$, as obtained by Korn and Braunstein processing the room-temperature absolute reflectivity spectrum shown in Fig. 3.

The extent to which this characteristic pattern can be evaluated in terms of type and location of critical points will depend upon a theoretical understanding and a subsequent analysis of the effect. The basis of such an analysis is provided by the relation between the periodic variation of temperature and the corresponding change of the density-of-states function induced in the neighborhood of critical points by this variation. The measured values of $\Delta R/R$ are related to the variation $\Delta\epsilon_1$ and $\Delta\epsilon_2$ of the real and imaginary parts of the complex dielectric constant by the well-known relation[18]:

$$\Delta R/R = \alpha(n,k)\Delta\epsilon_1 + \beta(n,k)\Delta\epsilon_2 \ . \tag{6}$$

On the other hand, the quantities $\Delta\epsilon_1$, and $\Delta\epsilon_2$, whose physical meaning is more direct, may be deduced from the experimental values of $\Delta R/R$ by means of the Kramers-Kronig dispersion relations.

The values of n and k, necessary for this computation, are shown in Fig. 4 as obtained by Korn and Braunstein processing the experimental absolute reflectivity curve shown in Fig. 3. As it is shown in Eq. (6), the overlapping of the contributions of $\Delta\epsilon_1$, and $\Delta\epsilon_2$ to give the experimental results for $\Delta R/R$, may generate accidental structures in $\Delta R/R$, not directly correlated to band-structure critical points. Before proceeding to a discussion of the experimental results we will separate these terms by performing a Kramers-Kronig analysis of $\Delta R/R$ to extract from it the $\Delta\epsilon_1$, and $\Delta\epsilon_2$ quantities.

If we represent the complex amplitude of reflection r by $r = R^{1/2}e^{i\theta}$, the phase angle θ is related to the normal incidence reflectivity R through the Kramers-Kronig relation:

$$\theta(\omega) = \frac{2\omega}{\pi} \mathcal{P}\int_0^\infty \frac{\ln R(\omega)}{\omega'^2 - \omega^2}\, d\omega' \ . \tag{7}$$

By differentiation with respect to temperature we obtain:

$$\frac{\Delta\theta(\omega)}{\Delta T} = \frac{2\omega}{\pi} \mathcal{P}\int_0^\infty \frac{1}{R}\frac{\Delta R}{\Delta T}\frac{d\omega'}{\omega'^2 - \omega^2} \ . \tag{8}$$

This integral can be transformed[29] into

$$\frac{\Delta\theta(\omega)}{\Delta T} = \frac{1}{2\pi}\left[\left(\frac{1}{R}\frac{\Delta R}{\Delta T}\right)_{\omega=\omega_1} \ln\frac{\omega+\omega_1}{\omega-\omega_1} - 2\omega\int_{\omega_1}^{\omega-\Delta\omega} \frac{1}{R}\frac{\Delta R}{\Delta T}\frac{d\omega'}{\omega'^2-\omega^2} + \left(\frac{1}{R}\frac{\Delta R}{\Delta T}\right)_{\omega=\omega_2} \ln\frac{2\omega-\Delta\omega}{2\omega+\Delta\omega} - 2\omega\int_{\omega+\Delta\omega}^{\omega_2} \frac{1}{R}\frac{\Delta R}{\Delta T}\frac{d\omega'}{\omega'^2-\omega^2}\right] \tag{9}$$

where $\hbar\omega_1$ and $\hbar\omega_2$ are the limits of the experimental energy range. The value of $\hbar\Delta\omega$ used was chosen such that the error in $\Delta\theta/\Delta T$ was about 0.1%. The corresponding changes $\Delta\epsilon_1$ and $\Delta\epsilon_2$ can be evaluated from the experimental values of $(1/R)(\Delta R/\Delta T)$ and the computed values of $\Delta\theta/\Delta T$ taking into account the expressions relating the optical constants ϵ_1 and ϵ_2 to R and θ.

Since Kramers-Kronig relations call for integration from 0 to ∞, extrapolation techniques have to be generally used to extend $\Delta R/R$ beyond the rather narrow experimental range of energies. However, due to the sharpness of the $\Delta R/R$ lines, contributions of the extrapolation region to $\Delta\theta$ are nonsingular and limited to the immediate neighborhood of critical points. Hence the extrapolation is not necessary, $\Delta\epsilon_1$ and $\Delta\epsilon_2$ are obtained with the expressions

$$\begin{aligned}\Delta\epsilon_1 &= A_1(\epsilon_1, \epsilon_2)\Delta R/R + A_2(\epsilon_1, \epsilon_2)\Delta\theta\ ,\\ \Delta\epsilon_2 &= -\tfrac{1}{2}A_2(\epsilon_1, \epsilon_2)\Delta R/R + 2A_1(\epsilon_1, \epsilon_2)\Delta\theta\ .\end{aligned} \tag{10}$$

This computation was carried out for all the experimental data, using the computed values of ϵ_1 and ϵ_2 to deduce the coefficients A_1 and A_2.

The computed values $\Delta\epsilon_1$ and $\Delta\epsilon_2$ obtained processing the room-temperature thermoreflectance spectrum of Fig. 3 are shown in Fig. 5. In Fig. 6 the obtained spectral dependence of the fractional coefficients α and β of Eq. (6) are shown. In order to achieve a phenomenological interpretation of the observed experimental results we focused our attention on the spectral dependence of the change of the imaginary part $\Delta\epsilon_2$ of the dielectric function induced by the temperature modulation of the sample, this quantity being the more strictly correlated to the theory of the optically induced direct interband transitions, as sketched in Sec. II. As is evident from Fig. 5, a strong dispersionlike line shape in $\Delta\epsilon_2$ appears in correspondence with the strong negative peak (E_2) present in the thermoreflectance spectrum in the neighborhood of 2.3 eV, followed by weaker structure corresponding to the E_3 and E_4 peaks, present also in the thermoreflectance spectrum. Structures in $\Delta\epsilon_1$ and $\Delta\epsilon_2$ are typically shifted down in energy from the reflectivity $\Delta R/R$ spectrum.

Korn and Braunstein, in their analysis of wavelength-modulated reflectance line shapes of the complete $Pb_xSn_{1-x}Te$ alloy series, attribute the strong E_2 transition to accidentally degenerate M_1 and M_2 singularities along Δ and Σ axes in the Brillouin zone as predicted by the recent band-structure calculations of Herman *et al.*[14] For the sample composition we are interested in, these authors found a critical point energy of 2.33 eV at 80 K. Rabii and Fischer[22] compared, however, the same experimental results with only the exact M_1 theoretical line shape for the appropriate ω_g, normalized to make the theoretical and experimental negative peaks in $d\epsilon_1/d\omega$ coincide, concluding that a pure M_1 singularity was not a bad assumption for the origin of this transition, calling into ques-

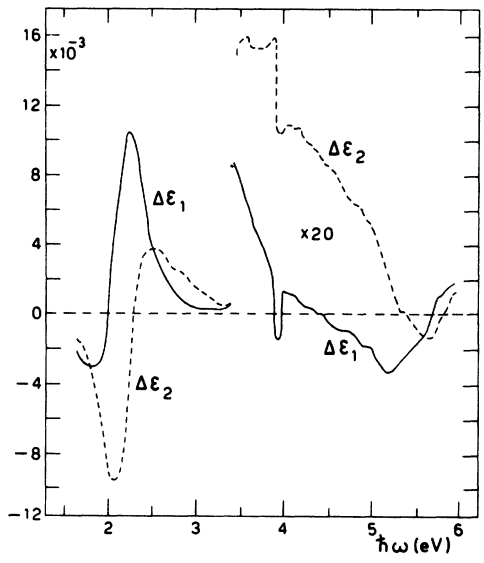

FIG. 5. $\Delta\epsilon_1$ (solid line) and $\Delta\epsilon_2$ (dashed line) for $Pb_{0.83}Sn_{0.17}Te$ at room temperature as obtained from the Kramers-Kronig analysis of the data of Fig. 3.

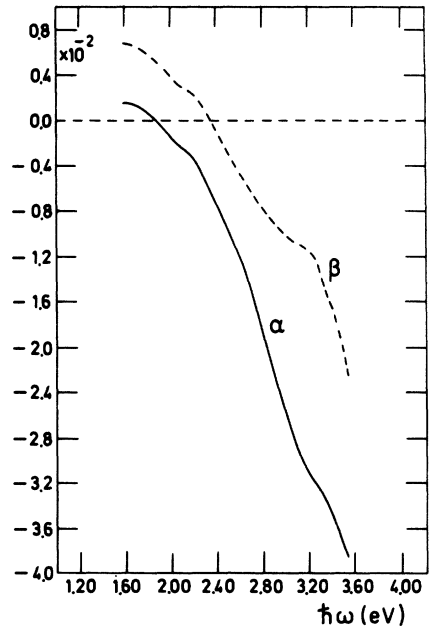

FIG. 6. Fractional coefficients $\alpha(n,k)$ and $\beta(n,k)$, calculated from the values of n and k of Korn and Braunstein (Ref. 21).

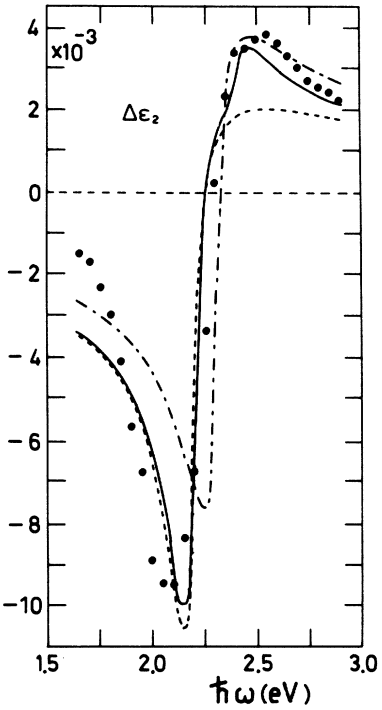

FIG. 7. Comparison between the experimental temperature-induced change in ϵ_2 for $Pb_{0.83}Sn_{0.17}Te$ at room temperature (black points) and the change calculated for a pure M_1 critical point (dashed line), an accidental degeneracy of M_1 and M_2 singularities (dot-dashed line), a nondegenerate overlapping of M_1 and M_2 critical points (solid line).

tion the possibility to extract numerical values from detailed curve fits to the approximate derivative functions. Focusing our attention on the E_2 region, a nonlinear least-squares curve-fitting technique based on the Rosenbrock[30] method has been used by us to compare our $\Delta\epsilon_2$ experimental results and the theoretical line shapes obtained by application of the exact derivative procedure outlined in Sec. II. We studied three distinct cases, corresponding to (i) a pure M_1 critical point, (ii) an accidental energy degeneracy of M_1 and M_2 singularities, and (iii) an overlapping contribution of M_1 and M_2 critical points positioned at different energies.

The free parameters $(\omega_g)_{M_1}$, $(\omega_g)_{M_2}$, Γ_{M_1}, and Γ_{M_2} were varied by the computer in order to minimize the rms error function. The results of this fitting procedure are shown in Fig. 7. Critical-point energies and Γ values obtained in the three cases are summarized in Table I. It is easily seen that the best fit of the experimental $\Delta\epsilon_2$ results is obtained at a temperature of 300 K, assuming the existence of nondegenerate M_1 and M_2 critical points.

We gave up trying to quantitatively describe the remaining weaker structure in $\Delta\epsilon_2$ because they seemed to us too vague for a definite assignment; their energy positions are, however, in reasonable agreement with those reported by Korn and Braunstein in wavelength-modulation reflectivity measurements.

Displayed in Fig. 3 is the nominally liquid-nitrogen temperature (actually 100 K) $\Delta R/R$ spectrum obtained on the temperature-modulation spectrometer. Many peaks and structures appear which had no observable correlation with the room-temperature absolute and temperature-modulated reflectance spectra. The more striking differences are related to (i) the appearance of a doublet in the region of the E_2 peak, (ii) the existence of many more structures in the 3.5–4.5 energy region, and (iii) the disappearing of the strong positive maximum at about 5.5 eV present in room-temperature measurements.

A formal Kramers-Kronig analysis was not undertaken due to the inherent difficulties in interpreting $\Delta\epsilon_1$ and $\Delta\epsilon_2$ line shapes obtained by the complicated low-temperature $\Delta R/R$ spectrum and to the lack of knowledge of the spectral dependence of the optical constants of the $Pb_{0.83}Sn_{0.17}$ Te films at the measured temperature.

The temperature dependence of the energy positions of the prominent structures in thermoreflectance spectra was measured. The E_2 peak of $Pb_{0.83}Sn_{0.17}Te$ had a positive temperature coefficient dE_2/dT of about $(2.8 \pm 0.5) \times 10^{-4}$ eV/K, in good agreement with the value obtained by Korn and Braunstein. The temperature coefficient for the E_3 peak was reported to be practically zero,[21]

TABLE I. Critical-point energies (ω_g) and broadening parameter values (Γ) obtained by the fitting procedure used to obtain the results displayed in Fig. 7.

Critical point assignments	$(\omega_g)_{M_1}$ (eV)	$(\omega_g)_{M_2}$ (eV)	Γ_{M_1} (meV)	Γ_{M_2} (meV)
M_1	2.17	...	50	...
M_1+M_2	2.28	2.28	53	53
M_1, M_2	2.16	2.43	51	52

and this could explain the small relevance of this structure to the thermoreflectance spectrum (a shoulder clearly visible only in the low-temperature measurements at about 3.5 eV). On the contrary a very large negative temperature coefficient $(-1.7 \pm 0.5) \times 10^{-3}$ eV/K was observed for the structure positioned at about 5.5 eV.

V. CONCLUSIONS

Epitaxial layers of lead chalcogenides have been extensively studied following the demonstration by Zemel *et al.*[31] that growth on alkali halides gave films with bulklike optical properties and large carrier mobilities. Bogacki *et al.*[32] performed thermoreflectance measurements on epitaxially grown thin films similar to those described by Zemel, but only for the extremal composition values $x=0$ and $x=1$. Holloway *et al.*[33] have shown that growth on the fluorite-structure substrate BaF_2 yields IV-VI layers with exceptional quality. These layers are truly single-crystalline and the improvement in the quality is reflected in larger low-temperature mobilities.

We measured and studied for the first time the temperature-modulated reflectance spectrum (up to photon energies of 6 eV) of epitaxial single-crystal films of the $Pb_{0.83}Sn_{0.17}Te$ pseudobinary alloy obtained on (111) BaF_2 substrates by a multicathode radio-frequency–sputtering system. Low-temperature spectra resulted in much richer structures than previously reported thermoreflectance spectra obtained on films similar to those grown by the Zemel technique, and than wavelength-modulation-derivative reflectivity spectra of (100) Czochralski-grown bulk samples of $Pb_xSn_{1-x}Te$.

In the E_2 reflectivity peak region, a quantitative line-shape analysis of the derivative spectra $\Delta\epsilon_2$ has been performed using the exact procedure of derivative of interband dielectric function at Van Hove singularities. One of the most striking differences found between the approximate universal line-shape functions and the exact results obtained by including the nonresonant terms is that wavelength and temperature modulation no longer have identical line shapes. Our derivative spectra $d\epsilon_1/d\omega_g$ and $d\epsilon_2/d\omega_g$ are actually quite similar to those obtained by Bogacki *et al.*[32] while they are substantially different from the $d\epsilon_1/d\omega$ and $d\epsilon_2/d\omega$ functions computed by Korn and Braunstein. The fitting procedure used has moreover clearly indicated that two saddle-point singularities give rise to the main E_2 structure, according to recent band-structure calculations.

Positive temperature coefficients were measured in good agreement with those previously reported except for the structure at about 5.5 eV, where a large negative coefficient was measured.

---

*L. E. S. S., Via Cineto Romano, 42—00156 Roma, Italy.
†I. S. S., Viale Regina Elena, 299—00161 Roma, Italy.

[1]R. Dalven, in *Solid State Physics Advances in Research and Applications*, edited by F. Seitz and D. Turnbull (Academic, New York, 1973), Vol. 28, p. 179.
[2]W. W. Scanlon, in *Solid State Physics*, edited by F. Seitz and D. Turnbull (Academic, New York, 1959), Vol. 9, p. 83.
[3]Yu. V. Mol'tsev, E. D. Nensberg, A. V. Petrov, S. A. Semiletov, and Yu. I. Ukhanov, Fiz. Tverd. Tela 8, 2154 (1966) [Sov. Phys.-Solid State 8, 1713 (1967)].
[4]M. Cardona and D. L. Greenaway, Phys. Rev. 133, A1685 (1964).
[5]R. B. Schoolar and J. R. Dixon, Phys. Rev. 137, A667 (1965).
[6]E. D. Palik, D. L. Mitchell, and J. N. Zemel, Phys. Rev. 135, A763 (1966).
[7]P. J. Stiles, E. Burstein, and K. N. Langenberg, in *Proceedings of the International Conference on the Physics of Semiconductors, Exeter, 1962* (Physical Society, London, 1962).
[8]G. F. K. Garlick, in *Proceedings of the Seventh International Conference on the Physics of Semiconductors, Paris*, 1964 (Academic, New York, 1964) Vol. IV; and E. R. Washwell and K. F. Cuff., *ibid.*
[9]J. M. Besson, J. F. Butler, A. R. Calawa, W. Paul, and R. H. Rediker, Appl. Phys. Lett. 7, 206 (1965).
[10]W. E. Spicer and G. J. Lapeyre, Phys. Rev. 139, A565 (1965).
[11]J. B. Chonklin, Jr., L. E. Johnson and G. W. Pratt, Phys. Rev. 137, A1282 (1965).
[12]P. J. Lin and L. Kleinman, Phys. Rev. 142, 478 (1966).
[13]S. Rabii, Phys. Rev. 182, 821 (1969).
[14]F. Herman, R. L. Kortum, I. B. Ortenburger, and J. P. Van Dyke, J. Phys. Suppl. 29, C4-52 (1968).
[15]S. Rabii, Phys. Rev. 182, 821 (1969).
[16]Y. W. Tung and Marvin L. Cohen, Phys. Rev. 180, 823 (1969).
[17]S. E. Kohn, P. Y. Yu, Y. Petroff, Y. R. Shen, Y. Tsang, and M. L. Cohen, Phys. Rev. B 8, 1477 (1973).
[18]M. Cardona, Solid State Phys. Suppl. 11, 105 (1969).
[19]B. Batz, Semicond. Semimet. 9, 315 (1972).
[20]B. O. Seraphin, J. Phys. Suppl. 29, C4-95 (1968).
[21]D. M. Korn and R. Braunstein, Phys. Rev. B 5, 4837 (1972).
[22]S. Rabii and J. E. Fischer, Surf. Sci. 37, 576 (1973).
[23]G. Mondio, G. Saitta, and G. Vermiglio, Can. J. Phys. 53, 1664 (1975).
[24]M. Grandolfo, F. Somma, and P. Vecchia, Phys. Rev. B 5, 428 (1972).
[25]C. Corsi, I. Alfieri, and G. Petrocco, Infrared Phys. 12, 271 (1972).
[26]C. Corsi, I. Alfieri, and G. Petrocco, Appl. Phys.

Lett. 24, 484 (1974).
[27]See, for example, G. F. Bassani, in *Proceedings of the International School of Physics, Varenna, Course XXXIV*, edited by J. Tauc (Academic, New York, 1966).
[28]Y. Toyozawa, M. Inoue, M. Okazaki, and E. Hanamura, J. Phys. Soc. Jpn. 22, 1337 (1967).
[29]A. Frova, P. J. Boddy, and Y. S. Chen, Phys. Rev. 157, 700 (1967).
[30]H. H. Rosenbrock, Comput. J. 3, 175 (1960).
[31]J. N. Zemel, in *Solid State Surface Science*, edited by M. Green (Dekker, New York, 1969); J. N. Zemel, J. D. Jensen, and R. B. Schoolar, Phys. Rev. 140, A330 (1965).
[32]F. J. Bogacki, A. K. Sood, C. Y. Jang, S. Rabii, and J. E. Fischer, Surf. Sci. 37, 494 (1973).
[33]H. Holloway, E. M. Logothetis, and E. Wilkers, J. Appl. Phys. 41, 3543 (1970).